WORLD CONFERENCE ON TIMBER ENGINEERING 2025
BRISBANE, AUSTRALIA
Advancing Timber for the Future Built Environment

# SEISMIC PERFORMANCE EVALUATION OF CLT BALLOON-TYPE SHEAR WALLS WITH HIGH-CAPACITY DOWELED AND SCREWED HOLD DOWNS

Amir Ghahremani Baghmisheh [1], T.Y. Yang [2], Marjan Popovski[3], Jasmine B.W. McFadden[4], Zhiyong Chen[5], and Minghao Li[6]

**ABSTRACT:** There has been an increased focus on the lateral performance of balloon-type mass timber walls due to the growing recognition of the advantages of balloon construction in mid to high-rise timber buildings. This paper evaluates and compares the seismic performance of mid- to high-rise CLT balloon-type shear wall archetypes, focusing on the differences between high-capacity hold-downs that use dowels and hold-downs that use mixed angle self-tapping screws (STS). Several archetypes are designed considering different parameters, including archetype height, seismicity level, and hold-down type. Robust finite element models are developed in Abaqus software to capture the complex nonlinear behavior at the base of rocking CLT walls. Subsequently, nonlinear finite element models of the prototypes are developed using OpenSees Software. The rocking base behavior is calibrated using the results of the robust model subjected to pushover analysis. The nonlinear hysteresis behavior of high-capacity hold-downs with mixed angle STS and dowels is verified using available test data. The seismic performance of archetypes is investigated by employing the FEMA-P695 procedure. A suite of ground motions suitable for the sites is selected and incrementally scaled. Then, a series of incremental dynamic analyses (IDAs) are conducted to quantify the adjusted collapse margin ratio (ACMR). Results show the sufficiency of most of archetypes by comparing ACMR with the acceptable limits recommended by FEMA-P695 and highlight slightly better performance of hold downs with dowels compared to hold-downs with STS.

**KEYWORDS:** CLT Shear Walls, Balloon-Type Construction, High-Capacity Hold-Downs, Seismic Performance, IDA

[1] Amir Ghahremani Baghmisheh, Department of Civil Engineering. The University of British Columbia, Vancouver, Canada, amirghb73@gmail.com

[2] T.Y. Yang, Department of Civil Engineering. The University of British Columbia, Vancouver, Canada.

[3] Marjan Popovski, Building Systems Group, FPInnovations, Vancouver, Canada.

[4] Jasmine B.W. McFadden, National Research Council Canada, Ottawa, Canada.

[5] Zhiyong Chen, Building Systems Group, FPInnovations, Vancouver, Canada.

[6] Minghao Li, Department of Wood Science, The University of British Columbia, Vancouver, Canada.

https://doi.org/10.52202/080513-0178

## 1 – INTRODUCTION

Cross-laminated timber (CLT) is an engineered wood product suitable for wall applications. There are two primary construction methods for CLT wall buildings: the platform-type and the balloon-type methods. In high seismicity regions, platform-type mass timber walls, as a Seismic Force Resisting System, are limited to a height of 20 meters under NBCC 2020 [1]. However, there are no seismic design provisions in North America for balloon-type CLT shear walls as a lateral force-resisting system. The two main challenges preventing their inclusion are the lack of connection data and the determination of response modification factors, which engineers require for design. This paper presents the seismic design and evaluation of mid- to high-rise CLT balloon-type shear wall archetypes featuring high-capacity hold-downs with dowels and mixed-angle STS. The adequacy of these archetypes is assessed through advanced static and dynamic analyses, as well as collapse risk evaluation.

## 2 – BACKGROUND

Platform-type shear walls consist of multiple CLT panels, each spanning a single story. In contrast, balloon-type shear walls are constructed using CLT panels that extend across multiple stories. Compared to platform-type walls, balloon-type CLT shear walls offer several advantages, including efficient panel use, minimizing perpendicular-to-grain shrinkage, reducing high perpendicular-to-grain compressive stresses in CLT floor panels, and decreasing the number of required metallic connections.

While extensive research has been conducted on platform-type CLT shear walls [2–4], studies on balloon-type CLT walls remain limited. Li et al. [5] conducted cyclic tests on CLT balloon-type shear walls, including single cantilever, multi-panel, and hybrid coupled walls, exploring three different height-to-length aspect ratios (0.52, 1.3, and 3.3) with bolted and mixed-angle STS hold-downs. Chen and Popovski [6] performed monotonic and cyclic tests on balloon-type CLT shear walls measuring 4.1 m × 0.8 m, connected to the foundation using 90-degree self-tapping screws (STS) and steel brackets. Shahnewaz et al. [7] experimentally investigated the behavior of half-scale, two-storey high balloon-type coupled panel CLT walls with four different ledgers at mid-height. Blomgren et al. [8] conducted shake table tests on a full-scale, two-storey mass timber building with coupled panel balloon-type CLT shear walls as the lateral system. The coupled panel wall featured replaceable inter-panel steel plates as sacrificial energy dissipators and central threaded anchor rods at the base to resist uplift.

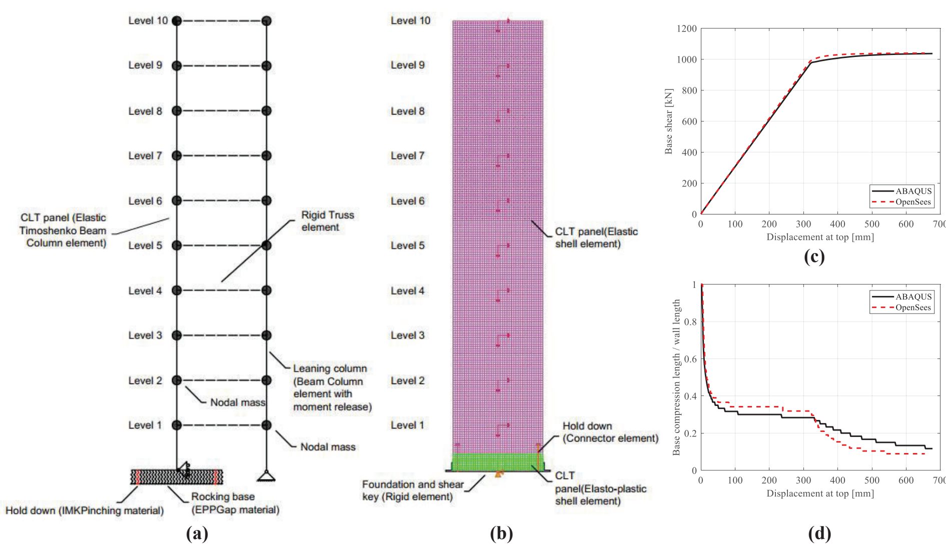


*Fig. 1: Schematic view of the(a) simplified model and (b) detailed model along with comparison of (c) base shear-top displacement curves and (d) base compression length variation curves of detailed and simplified model.*

As observed, most experimental tests on balloon-type CLT shear walls have focused on relatively low aspect ratios (less than 4), whereas mid-to-high-rise applications are expected to involve larger aspect ratios.


https://doi.org/10.52202/080513-0178

Beyond experimental studies, several researchers have

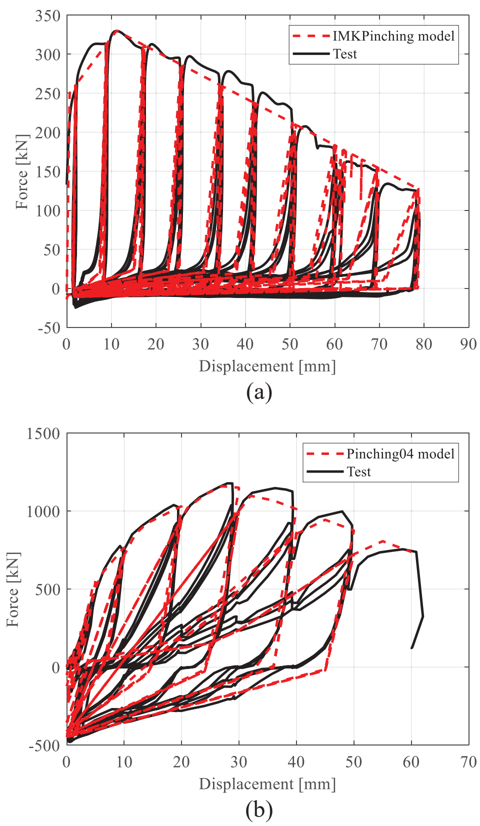


*Fig. 2: Comparing numerical force-displacement behaviour of (a) mixed angle STS and (b) and doweled hold-down with corresponding tests.*

investigated the performance of balloon-type walls using analytical models and numerical simulations. Jin et al. [9] developed a simplified mechanics-based analytical model to predict the pushover backbone curve and the sequence of limit states for coupled CLT panel walls, providing an alternative to finite element modeling. Chen and Popovski [6] introduced two analytical models—the rigid-base model and the elastic-base model—to predict the resistance and deflection of single and coupled balloon-type CLT shear walls under distributed static lateral loads. Pan et al. [10] examined the seismic performance of a two-storey balloon-type CLT school building in Vancouver using a 3D numerical model and conducted incremental dynamic analysis (IDA).

Additionally, several studies have explored the seismic performance of balloon-type CLT walls incorporating innovative energy-dissipative devices as hold-downs, such as buckling-restrained brace hold-downs [11,12] and resilient slip friction hold-downs [13].

Despite these efforts, previous studies have been limited to a small number of archetypes. A comprehensive study considering various conventional balloon-type archetypes with different influencing parameters is still lacking in the literature. This research gap provides challenges for designers, as no specific design guidelines exist for balloon-type CLT shear walls in building codes. Furthermore, there is a need to evaluate the adequacy of designed balloon-type CLT wall archetypes by quantifying their collapse margin ratio.

## 3 – METHODOLOGY

This section outlines the seismic evaluation procedure for balloon-type CLT shear wall archetypes followed in this paper. Since building codes do not provide design guidelines for balloon-type CLT shear walls, an equivalent static force-based (ESFP) seismic design approach was adopted using assumed response modification factors to design the archetypes. The adequacy of this design procedure was assessed through dynamic analyses.

A range of archetypes with varying numbers of stories, aspect ratios, seismic demands, and hold-down types were defined and designed using the procedure outlined in the subsequent section. Robust and detailed finite element models of the balloon-type walls were developed in Abaqus to accurately capture the complex behavior at the base of the walls. These models were then used to calibrate the base behavior of simplified models in OpenSees using spring elements. The nonlinear hysteresis behavior of high-capacity hold-downs with dowels and mixed angle STS was also calibrated based on previous connection test data.

The verified numerical modeling procedure was employed to develop 2D numerical models of the archetypes in OpenSees. To implement the FEMA-P695 [14] procedure, a suite of ground motions appropriate for the site and seismicity of the archetypes' location was selected and incrementally scaled, using spectral acceleration at the fundamental period as the intensity measure. IDAs were conducted to determine the intensity at which ground motions lead to system failure.

The results were used to derive collapse fragility curves and collapse margin ratios (CMR). Spectral shape factors (SSF), adjusted for the selected ground motions, were applied to obtain the adjusted collapse margin ratio (ACMR) for all archetypes.

https://doi.org/10.52202/080513-0178

## 4 – ARCHETYPES DESIGN

A total of 12 archetypes with single balloon-type CLT shear walls were designed in this study. The archetypes were categorized into four performance groups, each containing 6-, 8-, and 10-storey buildings located in either a extreme seismic zone (Seismic Category 4, Vancouver) or a high seismic zone (Seismic Category 3, Montreal) according to NBCC 2020 [1]. Each archetype featured hold-downs with either dowels or mixed angle STS connections. A typical residential floor plan with a 640-square-meter floor area was considered for all archetypes.

The assumed dead loads for the floor and roof were 2.8 kPa and 1.6 kPa, respectively. The live loads were 1.9 kPa for the floor and 1.0 kPa for the roof. Additionally, a 1-in-50-year ground snow load was considered for the site locations in Vancouver and Montreal. Most of the gravity load was resisted by the post-and-beam gravity system, while 20% of the gravity load was assigned to the lateral load-resisting walls.

All archetypes were assumed to be on Site Class D, with an average shear wave velocity of 250 $m/s^2$, in accordance with the NBCC 2020 [1] site classification. The CLT panels used in all archetypes were 9-ply thick, made of grade E1 material (Spruce-Pine-Fir MSR lumber), and had a 6-meter length (comprising two 3-meter-wide panels vertically joined with capacity-protected connections). The number of walls varied among archetypes depending on seismic demand.

The seismic design philosophy for the archetypes focused on ensuring that hold-down connections acted as the primary energy-dissipative components while capacity-protecting all other steel connections, including shear keys, vertical and horizontal joints, and wall-to-diaphragm connections. To achieve this, an appropriate capacity design factor was determined based on hold-down connection test results. The design capacities of the mixed-angle STS hold-downs tested by FPInnovations and doweled hold-downs tested by [15] were estimated using CSA O86-24 [16] provisions. The modified embedment strength from CSA O86 was used to predict the design force of the hold-downs with dowels and mixed angle STS. Since CSA O86 does not provide specific guidelines for designing mixed-angle STS hold-downs, a simple superposition of inclined and 90-degree screws was used to estimate the design capacity, as suggested in [17]. Overstrength factors of 3.0 and 2.5 were obtained for the hold-downs with mixed-angle STS and dowels, respectively, by dividing the peak force observed in tests by the design force. Note that design force of hold-down with mixed angle STS obtained using the modified embedment strength of CSA O86 resembling Eurocode 5 equation for embedment strength while design force of hold-down with dowels obtained using the embedment strength equation of CSA O86.

The ESFP was employed for the seismic design, assuming a ductility-related response modification factor ($R_d$) of 2 and an overstrength-related response modification factor ($R_o$) of 1.5 resulting in an R factor equal to 3. The empirical fundamental period prediction equation for wall systems ($T_a = 0.5h^{3/4}$) was used to estimate the design spectral acceleration and base shear demands, where $h$ is the height of the building. However, it is important to note that this equation was originally developed for concrete shear walls, whereas timber shear walls are significantly more flexible. To ensure that the numerical model period did not exceed twice the empirical code prediction, $2\times T_a$ was selected for the initial estimation of base shear and overturning moment demands.

The initial number of required walls was determined by comparing the factored shear and bending capacities of CLT panels computed using CLT handbook [18] with the seismic demands multiplied by the capacity design factor.

The hold-down design force was calculated based on the rocking wall system mechanics. In this method, an initial neutral axis depth (i.e., the compression length at the base of the rocking wall) was assumed, and the hold-down design force ($R_{t,hd}$) was estimated by taking moment equilibrium around the center of the CLT compression stress block, as shown in the equation below.

$$R_{t,hd} = \frac{\dfrac{M_u}{\phi} - N_g \times \left(\dfrac{L}{2} - \dfrac{L_p}{2}\right)}{L - L_{hd} - \dfrac{L_p}{2}} \qquad (1)$$

Where $M_u$ is the base overturning moment demand from the ESFP; $\phi$ is the resistance factor, taken as 0.9; $N_g$ is the gravity load imposed at the center of the wall; and $L$ is the wall length. $L_{hd}$ represents the distance from the center of the hold-down to the edge of the wall, while $L_p$ represents the plastic length at the base of the wall, i.e., the length of the wall panel where wood has reached its bearing capacity.

This equation assumes that the CLT has reached its bearing capacity under design-level forces and that the compression stress block at the base of the wall is rectangular. The plastic length is assumed to be 85% of the neutral axis depth, based on a parametric analysis of the


https://doi.org/10.52202/080513-0178

detailed Abaqus model of the wall, as presented in the next section.

*Table 1: Summary of archetypes designs*

| Archetype | Number of walls | Model first period (s) | Base shear per wall (kN) | Hold down design force (kN) |
|---|---|---|---|---|
| Mon-6-Story | 3 | 0.65 | 531 | 850 |
| Mon-8-Story | 3 | 1.01 | 448 | 888 |
| Mon-10-Story | 4 | 1.28 | 361 | 905 |
| Van-6-Story | 8 | 0.41 | 471 | 960 |
| Van-8-Story | 12 | 0.54 | 410 | 1150 |
| Van-10-Story | 16 | 0.7 | 334 | 1160 |

After calculating the hold-down design force, vertical force equilibrium was employed to verify the initial neutral axis depth assumption. An iterative process was conducted until the final neutral axis depth matched the assumed value.

A linear elastic model of the archetype was developed, and eigen analysis was performed to determine the fundamental period of the structure. The procedure for numerical model development is explained in the next section. Then, the ESFP demand was adjusted based on the model period.

If a practical ductile hold-down design could not be achieved for the obtained hold-down demand, the number of walls in the archetype was increased until a feasible hold-down design was possible. This process may require multiple iterations, as increasing the number of walls alters both the fundamental period of the structure and the seismic demand.

Design of hold-downs with dowels and mixed angle STS were completed using the provisions of CSA O86-24 [16]. To ensure ductile behavior, brittle failure modes were required to have a capacity greater than the ductile failure mode capacity multiplied by the capacity design factor. This limiting criterion governed the design of most archetypes, as brittle failure modes could not be practically protected for large hold-down design demands.

The final step of the design procedure involved checking inter-story drift. The total elastic lateral displacement, $\Delta_{Total}$, was obtained by summing the contribution of bending ($\Delta_{Bending}$), shear ($\Delta_{Shear}$), and rigid body rotation ($\Delta_{Rotation}$) of the wall as shown in Equation (2).

$$\Delta_{Total} = \Delta_{Bending} + \Delta_{Shear} + \Delta_{Rotation} \tag{2}$$

Note that it was assumed the shear keys were sufficiently rigid, preventing any sliding at the base of the wall under design-level forces. Bending and shear deformations were determined using mechanics-based formulas for cantilever beam deformation, as presented in [6]. The displacement corresponding to the rigid body rotation at each story level ($\Delta_{Rotation,i}$) was obtained using the following equation by assuming small deformations:

$$\Delta_{rot,i} = \frac{\delta_{hd}}{L - L_{hd} - L_c} \times h_i \tag{3}$$

Where $\delta_{hd}$ represents the elongation of the hold-down under design level forces, and $L$, $L_{hd}$, and $L_c$ denote the wall width, the distance from the hold-down center to the wall edge, and the compression base length, respectively. Finally, the elastic displacement was multiplied by $R_dR_o$ factor and checked against NBCC inter-storey drift limit. The design was revised if the drift limit was not satisfied. A summary of the designed archetypes including, model period, number of walls, maximum design base shear per wall in the N-S and E-W direction and hold down design force is presented in Table 1. Note that the design of archetypes having hold-downs with dowels and mixed angle STS is the same, so only the design summary of half of the archetypes is presented in Table 1.

## 5- NUMERICAL MODELING

This section describes the detailed and simplified modeling procedures for rocking CLT balloon-type walls. A detailed 2D model of a single wall (Fig. 1b) was developed in Abaqus software, where the CLT panel was simulated using shell elements with elastic orthotropic material properties. To account for possible nonlinearity at the base of a balloon-type CLT wall caused by high compression stress from rocking, a nonlinear material property was assigned to the bottom section of the wall. The hold-downs were modeled using connector elements with a simple elastic-perfectly plastic load-displacement behavior. Since pushover analysis was used to calibrate the base springs, a simplified backbone curve for the hold-down response was applied at this stage. The shear key and foundation were represented by rigid beam elements. Contact behavior was defined between the wall panel and foundation to simulate rocking behavior. More details on the modeling procedure and validation with experimental tests were presented in the authors' previous studies [19–21].

To obtain a computationally efficient model for numerous dynamic analyses, a simplified wall model (Fig. 1a) was developed in OpenSees software and calibrated with the detailed model. The wall panel was simulated using elastic Timoshenko beam elements, which are suitable for capturing both bending and shear deformations. Hold-downs were modeled using nonlinear zero-length elements. To replicate the rocking motion at the base of the wall, a set of uniformly distributed zero-length springs with elastic-perfectly-plastic gap material was employed. The stiffness properties of the base springs were tuned so that the pushover curves of the wall under a reversed triangular lateral load and the variation of the base compression length matched the results obtained from the detailed model (see Fig. 1c and Fig. 1d for an illustrative example of a 10-story archetype).

In addition to calibrating the base behavior of the simplified model, the hysteresis behavior of the hold-down connections was also verified against experimental tests. The IMKPinching and Pinching04 material models were used to simulate the hysteresis behavior of hold-downs with mixed angle STS and dowels, respectively, using zero-length elements in the simplified model. The cyclic curves of the connection models were compared with experimental cyclic curves in Fig. 2, showing a relatively good match between numerical simulations and experimental results. The verified modeling procedure was then employed to develop numerical models of the 12 archetypes in OpenSees software.

## 6- ANALYSIS RESULTS

This section presents the results of pushover analyses and IDAs required by the FEMA-P695 procedure to quantify the seismic performance of the archetypes. Pushover analyses were conducted on the archetypes using a reverse triangular load pattern corresponding to the lateral force distribution of ESFP, and base shear versus roof drift curves, known as pushover curves, were recorded. According to FEMA-P695 [14], the period-based ductility, $\mu_T$, is defined as the roof drift at which the shear load drops to 80% of the maximum shear load in the pushover curve, divided by the effective roof yield drift ($\Delta_{yeff}$). In this study, $\Delta_{yeff}$ is determined as the roof drift where the initial slope of the pushover curve intersects the peak shear load. These parameters are illustrated in the pushover curves presented in Fig. 3 for 8-storey archetypes in Vancouver having hold-downs with dowels and mixed angle STS as an example.

To conduct IDA, suites of ground motions (GMs) were selected for sites located in Vancouver and Montreal. The deaggregation analysis [12] showed that the Vancouver

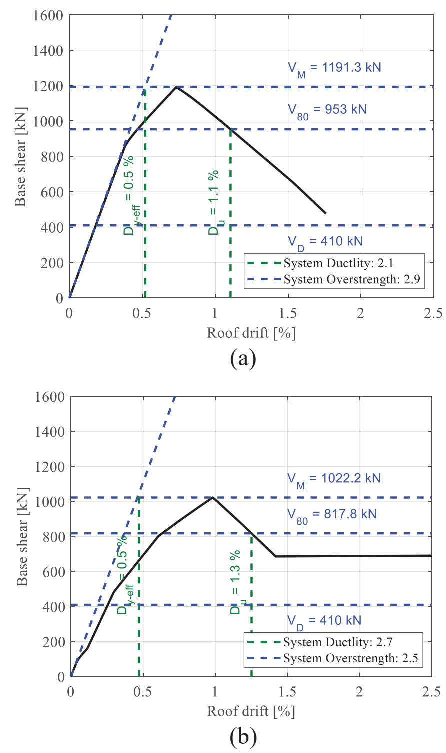


*Fig. 3: Pushover curves of 8 story archetype in Vancouver with (a) mixed angle STS and (b) doweled hold-downs*

site is influenced by three primary seismic hazard sources: crustal, inslab, and subduction interface earthquakes. In contrast, seismic hazard in Montreal is predominantly driven by crustal earthquakes. Thus, a suite of 33 GMs (11 GMs for each hazard source) was selected for the Vancouver site, and 11 GMs were selected for the Montreal site. Crustal GMs were obtained from the PEER NGA-West2 database [22], while the S2GM database [23] was employed to obtain inslab and interface GMs.

Spectral acceleration at the fundamental period of the archetypes was chosen as the intensity measure in the IDA. GMs were incrementally scaled and subjected to the model until system failure criteria were observed. The system failure criteria considered in this paper include: (1) Hold-down failure corresponding to the exceedance of the hold-down ultimate deformation capacity; (2) CLT panel shear failure corresponding to the exceedance of the in-plane


https://doi.org/10.52202/080513-0178

shear capacity of the panel; (3) CLT panel bending failure corresponding to the exceedance of the edge-wise bending capacity of the panel; (4) Horizontal joint failure corresponding to exceeding capacity of joint; (5) shar key failure corresponding to exceeding strength of shear key (6) Global instability corresponding to excessive roof drift (i.e., 5%); (7) Exceeding NBCC 2.5% drift criteria at 100% UHS intensity; Note that the maximum displacement observed in cyclic tests of the hold-downs with dowels was considered as the failure deformation for both hold-downs with dowels and mixed angle STS, even though hold-down with mixed angle STS sustained a larger maximum displacement as seen in Fig 2.

Fig. 4 shows the IDA results in terms of intensity measure versus roof drift for two archetypes as an example. Note that the vertical axis was normalized by dividing the spectral acceleration at the fundamental period by the spectral acceleration of the uniform hazard spectrum (UHS) at the fundamental period. UHS is associated with a 2% probability of exceedance in 50 years hazard for Site Class D ($V_{s30}$ = 250 m/s), according to NBCC 2020 [1]. Dots on the IDA curves of each GM represent the instance when the first failure criterion is met. As seen, hold-down failure was the most common reason for the collapse..

The collapse margin ratio is defined as the ratio of the shaking intensity at which the archetype has a 50% probability of collapse to the intensity of the uniform hazard spectrum. Seismic performance in FEMA-P695 is quantified in terms of the adjusted collapse margin ratio ACMR, where the CMR from IDA is adjusted based on the spectral shape factor. Since the ground motions used in this study differ from those in FEMA-P695, new SSFs were required to adjust the collapse margin ratio to the ACMR. In this study, the SSFs were determined using Equation (4) as outlined by [24].

$$SSF = \exp\left[\beta_1\left(\frac{\ln(CMR)}{\sigma_{GMM}}\right)\right] \tag{4}$$

Where $\beta_1$ is obtained from Equation (5) and $\sigma_{GMM}$ represents the logarithmic standard deviation of the ground motion prediction model obtained from [25] for crustal and from [26] for inslab and interface GMs.

$$\beta_1 = 0.14(\mu_T - 1)^{0.42} \tag{5}$$

Where period-based ductility ($\mu_T$) was obtained from pushover analyses. In order to calculate the total CMR for archetypes located in Vancouver with three hazard sources, CMR for each hazard source were weighted based on the hazard contribution resulting from hazard

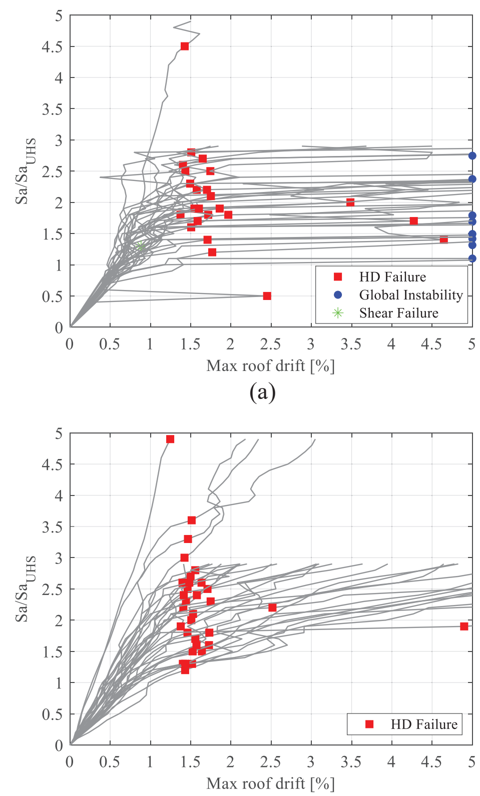


*Fig. 4: IDA curves of 8 story archetype in Vancouver with (a) mixed angle STS and (b) doweled hold-downs.*

deaggregation as outlined in [24]. Fig. 5a and Fig. 5b compare collapse fragility curves of the archetypes having hold-downs with mixed angle STS and dowels, respectively. ACMR values for all archetypes are summarized in Fig. 6. As seen, archetypes having hold-downs with dowels have slightly higher ACMR values relative to archetypes having hold-downs with mixed angle STS. This can be attributed to the greater energy dissipation capacity of doweled hold-downs when their cyclic curves are compared. Finally, the total ACMR was compared to the acceptable ACMR value of 1.90 specified in FEMA-P695 [14], which corresponds to a 10% probability of collapse and a total system collapse uncertainty of 50%. It was found that all archetypes except two 6-story archetypes satisfy the requirements of FEMA-P695 and provide sufficient margin against collapse. The lower ACMR value for the 6-story archetypes is attributed to premature shear failure of the CLT panel observed in several GMs instead of hold-down failure. This suggests that the design procedure should be revised for low aspect ratio archetypes to prevent premature shear failures. This can also be attributed to the assumed rigid shear key at the base of the wall in the numerical model which impose high shear load on the panel.

## 7- CONCLUSIONS AND RECOMMENDATIONS

This study presents a comprehensive seismic design and evaluation of balloon-type CLT shear walls for mid- to high-rise buildings. The research addresses the gap in design provisions for balloon-type CLT shear walls, proposing an equivalent static force-based design procedure coupled with advanced dynamic analyses to assess seismic performance. A series of 12 archetypes, varying in storey number, seismic zone, and hold-down types, were designed and analyzed using both detailed finite element models and simplified models in OpenSees. The results of the pushover analyses and incremental dynamic analyses were used to quantify the seismic performance of these archetypes, with a focus on the collapse margin ratio and adjusted collapse margin ratio as the primary performance indicators.

The findings indicate that archetypes having hold-downs with dowels generally exhibited slightly higher ACMR values compared to those having hold-downs with mixed angle STS, highlighting the greater energy dissipation capacity of the doweled hold-downs. Furthermore, the study demonstrated that all archetypes, except two 6-storey designs using STS hold-downs, satisfied the FEMA-P695 requirements, providing a sufficient margin against collapse. The lower ACMR values for the 6-storey archetypes were attributed to premature shear failure of the CLT panels, emphasizing the need for design revisions for low aspect ratio systems to prevent such failures.

This research contributes valuable insights to the design of balloon-type CLT shear walls, providing a foundation for future development of seismic design provisions and guidelines. The findings highlight the importance of ensuring robust capacity design procedures, particularly for buildings in high seismic regions, and the need for continued research to refine and optimize the seismic performance of balloon CLT shear wall system.

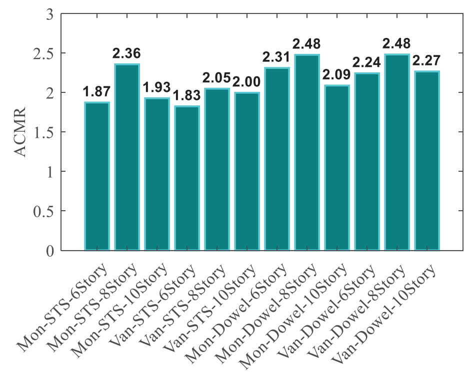


*Fig. 6: Summary of ACMR values for all the archetypes.*

## 8- REFRENCES


[1] NBCC. National Research Council of Canada (NRC). National Building Code of Canada 2020. 2020.

[2] D'Arenzo G, Schwendner S, Seim W. The effect of the floor-to-wall interaction on the rocking stiffness of segmented CLT shear-walls. Eng Struct 2021;249:113219.

[3] Kovacs MA, Wiebe L. Controlled rocking CLT walls for buildings in regions of moderate seismicity: Design procedure and numerical collapse assessment. J Earthq Eng 2019;23:750–70.

[4] Mugabo I, Barbosa AR, Sinha A, Higgins C, Riggio M, Pei S, et al. System identification of UCSD-NHERI shake-table test of two-story structure with cross-laminated timber rocking walls. J Struct Eng 2021;147:4021018.

[5] Li M, Moerman B, Wright T, Liu A. Seismic performance of multi-storey cross laminated timber shear walls with high-capacity anchoring systems. 2023.

[6] Chen Z, Popovski M. Mechanics-based analytical models for balloon-type cross-laminated timber (CLT) shear walls under lateral loads. Eng Struct 2020;208:109916.

[7] Shahnewaz M, Dickof C, Tannert T. Seismic behavior of balloon frame CLT shear walls with different ledgers. J Struct Eng 2021;147:4021137.

[8] Blomgren H-E, Pei S, Jin Z, Powers J, Dolan JD, van de Lindt JW, et al. Full-scale shake table testing of cross-laminated timber rocking shear walls with replaceable components. J Struct Eng 2019;145:4019115.

[9] Jin Z, Pei S, Blomgren H, Powers J. Simplified mechanistic model for seismic response prediction of coupled cross-laminated timber rocking walls. J Struct Eng 2019;145:4018253.

[10] Pan Y, Jafari M, Shahnewaz M, Tannert T. SEISMIC ASSESSMENT OF BALLOON-FRAMED CROSS-LAMINATED TIMBER



https://doi.org/10.52202/080513-0178

SCHOOL BUILDING 2022.

[11] Tesfamariam S, Teweldebrhan BT. Seismic Design of Tall Timber Building with Dual CLT-Shear Wall and Glulam Moment Resisting Frame Systems 2023.

[12] Yang TY, Lepine-Lacroix S, Guerrero JAR, McFadden JBW, Al-Janabi MAQ. Seismic performance evaluation of innovative balloon type CLT rocking shear walls. Resilient Cities Struct 2022;1:44–52.

[13] Hashemi A, Masoudnia R, Quenneville P. A numerical study of coupled timber walls with slip friction damping devices. Constr Build Mater 2016;121:373–85.

[14] FEMA-P695. FEMA P695 , Quantification of building seismic performance factors. 2009. https://doi.org/10.1016/j.compstruc.2009.08.001.

[15] Ottenhaus L-M, Li M, Smith T. Structural performance of large-scale dowelled CLT connections under monotonic and cyclic loading. Eng Struct 2018;176:41–8.

[16] CSA-O86. Canadian Standards Association (CSA Group). CSA O86-24: Engineering design in wood. 2024. 2024.

[17] Wright T, Li M, Carradine D, Moroder D. Cyclic behaviour of hold-downs using mixed angle self-tapping screws in Douglas-fir CLT 2021.

[18] Karacabeyli E, Gagnon S. Canadian CLT handbook. 2019.

[19] Chen Z, Cuerrier-Auclair S, and Popovski M. Advanced Wood-based Solutions for Mid-rise and High-rise Construction: Analytical Models for Balloon-Type CLT Shear Walls.FPInnovations Project (301012205) Report, Vancouver, Canada. 2018.

[20] Chen Z, Popovski M, Jackson R, Epp L, Software and D. "Chapter 7.2 – Mass Timber Structures." In Modelling Guide for Timber Structures. FPInnovations, Pointe-Claire, Canada., 2022.

[21] Chen Z, Popovski M. EXPANDING WOOD USE TOWARDS 2025: PRELIMINARY INVESTIGATION OF THE SEISMIC PERFORMANCE OF BALLOON-TYPE CLT SHEAR WALLS AND KEY SEISMIC DESIGN. FPInnovations Project (301014606) Report, Vancouver, Canada. FPInnovations Project (301014606) Report, Vancouver, Canada.; 2022.

[22] Kishida T, Contreras V, Bozorgnia Y, Abrahamson NA, Ahdi SK, Ancheta TD, et al. NGA-sub ground motion database. 2018.

[23] Bebamzadeh A, Ventura CE, Fairhurst M. S2GM: Ground motion selection and scaling database. Annu. Los Angeles Tall Build. Des. Counc. Meet. Los Angeles, CA, 2015.

[24] Bagatini-Cachuco F, Yang TY. Seismic performance assessment of pre-engineered steel buildings on the west coast of Canada. Steel Compos Struct An Int J 2021;41:461–74.

[25] Boore DM, Atkinson GM. Ground-motion prediction equations for the average horizontal component of PGA, PGV, and 5%-damped PSA at spectral periods between 0.01 s and 10.0 s. Earthq Spectra 2008;24:99–138.

[26] Abrahamson N, Gregor N, Addo K. BC Hydro ground motion prediction equations for subduction earthquakes. Earthq Spectra 2016;32:23–44.